Total Cross Sections for 410-Mev Neutrons*

V. ALEXANDER NEDZEL†
Physics Department and Institute for Nuclear Studies, University of Chicago, Chicago, Illinois
(Received December 21, 1953)

Good geometry transmission measurements were conducted in the high-energy neutron beam of the University of Chicago synchrocyclotron. Total cross sections of fourteen elements, measured at an effective neutron energy of 410 Mev, were determined as follows (units of millibarns):

Hydrogen	33.7±1.3	Chlorine	742±10
Deuterium	62.0±4	Iron	1073±12
Beryllium	231±4	Copper	1187±14
Carbon	297±3	Cadmium	1848±21
Oxygen	378±5	Lead	2890±30
Aluminum	587±8	Thorium	3210±40
Sulfur	672±9	Uranium	3230±40

It was found that the following two-parameter empirical formula was consistent with the measured cross sections to within the accuracy of their determination:

$$\sigma=2\pi R^2[1-\exp(-KR)],$$

where $R=r_0A^{\frac{1}{3}}$, and the two constants were chosen as $r_0=1.20\times10^{-13}$ cm, and $K=0.360\times10^{13}$ cm^{-1}. The sole exception was hydrogen, for which the prediction by the formula was 5 percent below the measured value.

The results are compared with neutron cross sections at lower energies, with proton cross sections at the same energy, and are discussed from the point of view of the transparent optical model.

I. INTRODUCTION

THE measurement of the total cross sections of nuclei for fast neutrons provides one of the best bases for the determination of nuclear radii. Knowledge of the dependence of these cross sections on energy and on mass number allows tests of various nuclear models.

For neutrons of greater energy than those at which resonances occur, the total cross sections would be expected to show a smooth dependence on mass number and on energy. Provided the energy of the neutrons is not so high that nuclei begin to show transparency effects, the theory of nuclear cross sections of Feshbach and Weisskopf[1] predicts asymptotically, for high energy and large R,

$$\sigma_t=2\pi(R+\lambda\!\!\!^{-})^2, \tag{1}$$

where R is the nuclear radius and λ the de Broglie wavelength of the incident neutron. In this limit, and assuming constant nuclear density, one would expect

$$(\sigma_t/2\pi)^{\frac{1}{3}}=a+r_0A^{\frac{1}{3}}, \tag{2}$$

where r_0 is the nucleon radius and a is independent of A but a function of the energy. The agreement with experimentally determined cross sections at 14 Mev[2–8] and at 25 Mev[9] is fair, at least as to over-all trend. Some of these data have been interpreted[1,7,10] to yield a value of about 1.5×10^{-13} cm for r_0.

Striking deviations from (1) and (2) were observed in measurements at 42 Mev,[11] at 83 Mev,[12,13] and at 95 Mev.[14] The transparent optical model of Fernbach, Serber, and Taylor[15] successfully interpreted the cross sections at 83 Mev, the best fit to the data occurring when the three parameters of the theory were chosen as follows: the nucleon radius, $r_0=1.38A^{\frac{1}{3}}\times10^{13}$ cm^{-1}; the increase in wave number of the neutron wave upon entering the nucleus, $k_1=0.285\times10^{13}$ cm^{-1}; and the absorption coefficient of the neutron wave in nuclear matter, $K=0.30\times10^{13}$ cm^{-1}.

At the still higher energy of 153 Mev,[16] and particularly at 270 Mev[17] and 280 Mev,[18] the character of the dependence of the cross sections on mass number was found to change again. In order to apply the optical model to the latter two observations the constant k_1 had to be taken as zero, implying that the index of

* Assisted by a joint program of the U. S. Office of Naval Research and of the U. S. Atomic Energy Commission.
† Now at Lincoln Laboratory, Massachusetts Institute of Technology, Cambridge, Massachusetts.
[1] H. Feshbach and V. F. Weisskopf, Phys. Rev. **76**, 1550 (1949).
[2] Amaldi, Bocciarelli, Cacciapuoti, and Trabacchi, Nuovo cimento **3**, 203 (1946).
[3] A. H. Lasday, Phys. Rev. **81**, 139 (1951).
[4] D. I. Meyer and W. Nyer, Los Alamos Report LA-1279, 1951 (unpublished).
[5] Poss, Salant, and Yuan, Phys. Rev. **85**, 703 (1952).
[6] Ageno, Cortellessa, and Querzoli, Rend. reale accad. nazl. Lincei **13**, 253 (1952).
[7] Coon, Graves, and Barschall, Phys. Rev. **88**, 562 (1952).
[8] L. S. Goodman, Phys. Rev. **88**, 686 (1952).
[9] R. Sherr, Phys. Rev. **68**, 240 (1945).
[10] E. Amaldi and B. N. Cacciapuoti, Phys. Rev. **71**, 739 (1947).
[11] R. H. Hildebrand and C. E. Leith, Phys. Rev. **80**, 842 (1950).
[12] Cook, McMillan, Peterson, and Sewell, Phys. Rev. **75**, 7 (1949).
[13] Bratenahl, Fernbach, Hildebrand, Leith, and Moyer, Phys. Rev. **77**, 597 (1950).
[14] J. DeJuren and N. Knable, Phys. Rev. **77**, 606 (1950).
[15] Fernbach, Serber, and Taylor, Phys. Rev. **75**, 1352 (1949).
[16] Taylor, Pickavance, Cassels, and Randle, Phil. Mag. **42**, 20, 751 (1951).
[17] J. DeJuren, Phys. Rev. **80**, 27 (1950).
[18] Fox, Leith, Wouters, and MacKenzie, Phys. Rev. **80**, 23 (1950).

refraction of nuclear matter had become one for neutrons of these energies.

The dependence of the cross sections on the mass number A at these various energies is illustrated in Fig. 1. The variation of $(\sigma_t/2\pi)^{\frac{1}{2}}$, the effective nuclear radius, with $A^{\frac{1}{3}}$ is shown in Fig. 2.

Observations have also been made[19–21] of the cross sections of certain elements as functions of energy in the 30–200 Mev range. Taylor and Wood[22,23] discovered maxima in this energy range of the cross sections of several elements. This phenomenon has been interpreted by Lawson[24] as a diffraction effect demonstrating the transparency of nuclei to high-energy neutrons.

The rapid drop in cross sections between about 100 and 150 Mev can be understood in terms of the optical model if the index of refraction of nuclear matter is postulated to drop rapidly to one at these energies. This variation of the index is not predicted by the Fermi gas model (a discussion of this point, and of the optical

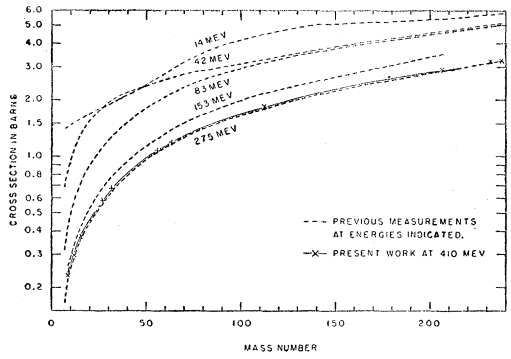

FIG. 1. Total cross sections are plotted as functions of the mass number for neutrons of the energies indicated. Except in the case of several of the lighter elements at 14 Mev, the actual experimental values fall within the estimated errors of the smooth curves drawn. The 14-Mev data used was that of reference 7.

model more generally, is given in Memmert).[25] This theoretical postulate, which implies that it is the coherent or elastic contribution to the total cross section that drops rapidly in this energy range, is supported by comparison of the observations of the elastic and inelastic cross sections at 95 Mev[14] with those at 300 Mev.[26] A theory more in accord with the observed variation of the index of refraction was proposed by Jastrow,[27] who calculated the index in terms of the forward scattering amplitudes of the nucleon-nucleon interactions using his "hard core" model.[28] Jastrow

[19] J. DeJuren and B. J. Moyer, Phys. Rev. **81**, 919 (1951).
[20] Taylor, Pickavance, Cassels, and Randle, Phil. Mag. **42**, 328 (1951).
[21] Mott, Guernsey, and Nelson, Phys. Rev. **88**, 9 (1952).
[22] A. E. Taylor and E. Wood, Phys. Rev. **87**, 907 (1952).
[23] A. E. Taylor and E. Wood, Phil. Mag. **44**, 95 (1953).
[24] J. D. Lawson, Phil. Mag. **44**, 102 (1953).
[25] G. Memmert, Z. Physik **134**, 42 (1952).
[26] W. P. Ball, University of California Radiation Laboratory Report UCRL-1938 (unpublished).
[27] R. Jastrow, Phys. Rev. **82**, 261 (1951).
[28] R. Jastrow, Phys. Rev. **81**, 636 (1951).

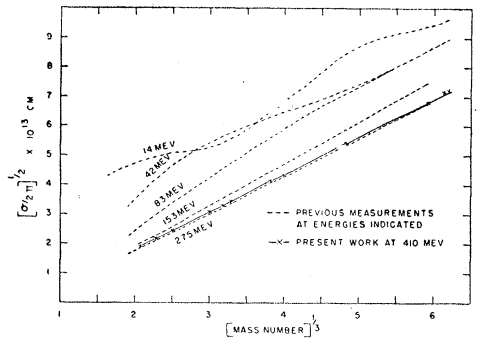

FIG. 2. Effective radii, $(\sigma/2\pi)^{\frac{1}{2}}$, are plotted as functions of $A^{\frac{1}{3}}$ for neutrons of the energies indicated. Except in the case of several of the lighter elements at 14 Mev, the actual experimental values fall within the estimated errors of the smooth curves drawn.

and Roberts[29] have proposed a nuclear model with a nonuniform density in order to better account for the variation of the neutron cross sections over the whole 14–270 Mev range. These various features of the energy dependence of total cross sections are shown in Fig. 3. In this compilation use was made of a previous summary.[30]

Since 280 Mev represents the highest energy at which total neutron cross sections have heretofore been measured, it was thought of importance to undertake the present study at the University of Chicago cyclotron where neutrons of over 400 Mev are available in considerable intensity. It appeared of especial interest to investigate whether the leveling off of the cross sections observed between 150 and 300 Mev extended

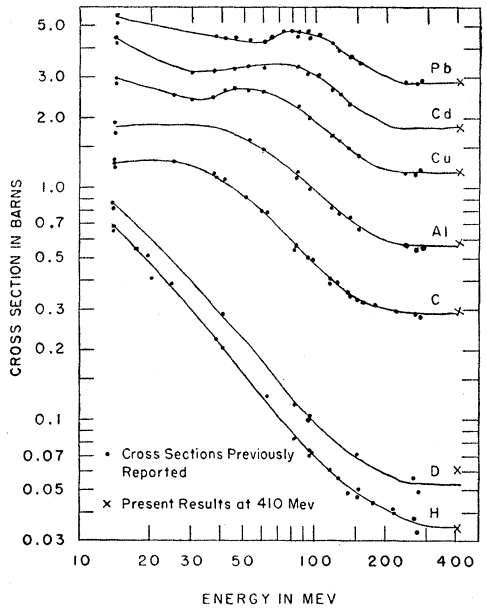

FIG. 3. Total cross sections of several elements as functions of neutron energy.

[29] R. Jastrow and J. E. Roberts, Phys. Rev. **85**, 757 (1952).
[30] Hildebrand, Hicks, and Harker, University of California Radiation Laboratory Report UCRL-1305, 1951 (unpublished).

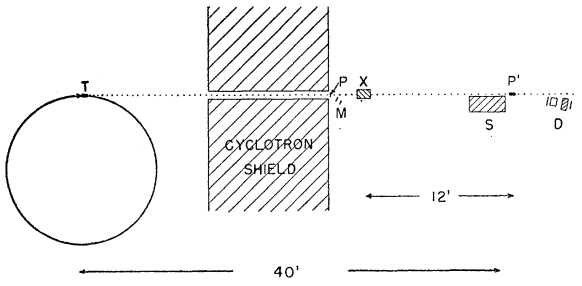

FIG. 4. The layout of the experiment. T represents the internal beryllium target; P and P' are the polyethylene scatterers for monitor and detector, respectively; S is an auxiliary shield for the detector; X is the sample (in beam attenuating position); and M and D represent monitor and detector telescopes.

to higher energies, and to compare the mass number dependence of the cross sections at 400 Mev with that at lower energies. To this end, fourteen elements were selected for study, as follows: hydrogen, deuterium, beryllium, carbon, oxygen, aluminum, sulfur, chlorine, iron, copper, cadmium, lead, thorium, and uranium. The cross sections of these elements were determined by good geometry transmission measurements, with the width of the effective neutron energy spectrum limited by the use of a proton recoil threshold detector.

Some of the results of this work have already been reported in preliminary form.[31,32]

II. APPARATUS AND PROCEDURE

A. Layout

The arrangement of the experiment is shown in Fig. 4. The source of neutrons is a 2-in. thick, 1-in. high beryllium target T placed in the circulating proton beam of the cyclotron at the 76-in. radius, where the nominal proton energy is 450 Mev. The neutrons emitted in the forward direction from this target are collimated in the twelve-foot thick steel shield wall that separates the cyclotron from the experimental area. The collimation was effected by two three-foot long steel plugs, one inserted into each end of the neutron channel through the shield wall. These plugs were bored appropriately to produce a beam 1 in. in diameter at the sample position X in the experimental area.

The beam intensity was monitored by the scintillation counter telescope M placed at an angle of 20° to the beam, where it observed recoil protons from a 1-in. thick sheet of polyethylene P placed in the beam. Neutrons not removed from the beam by the sample were incident upon a 1 in.×1 in.×5 in. polyethylene scatterer P'. The detector telescope D observed proton recoils from P' emitted at 10° to the neutron beam, while the steel shield S prevented particles scattered from the sample from reaching the counters of D directly.

The distance from the Be target to the sample was twenty-eight feet, while that from sample to detector scatterer was twelve feet. The detector scatterer subtended a solid angle of 4.8×10^{-5} steradian at the sample position.

B. Counters

The principal requirements of the counter systems were strict linearity and stability, maximum sensitivity to high-energy proton recoils from the polyethylene scatterers, and minimum sensitivity to radiation reaching the counters from other directions. In the case of the detector, it was also desired to have an absolute energy threshold for the counting of proton recoils.

The arrangement of the detector and monitor counters is shown in Fig. 5. The counters of the detector telescope are set along a line 10° off the direction of the neutron beam. This was done for two reasons: First, to get the counters out of the direct beam where they would be subject to neutrons, gamma rays, and electrons, as well as to the recoil protons, which would create the disadvantage of increasing the singles rates in the counters; second, to permit the counters to be shielded from particles scattered from the sample directly.

In Fig. 5, A and B are scintillation counters 3.5 in. and 5.5 in. in diameter, set 24 in. and 38 in. back, respectively, from the scatterer P. Both counters use liquid scintillators, consisting of saturated solutions of terphenyl in phenyl-cyclohexane, viewed by 5819 photomultiplier tubes. C is a nonfocusing Čerenkov radiation counter, of the general type described by Marshall,[33] consisting of a 4-in. thick Lucite radiator mounted in the axis of the telescope and covering the 4.25 in.×3.125 in. photocathode of the RCA developmental type C7157 photomultiplier tube against which it is fastened.

A Čerenkov radiation counter was selected for use in the detector because it has a natural threshold (the

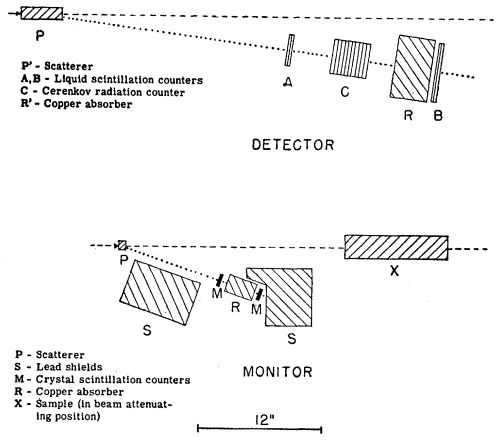

FIG. 5. The detector and monitor telescope arrangement.

[31] V. A. Nedzel and J. Marshall, Phys. Rev. **86**, 604 (1952).
[32] V. A. Nedzel, Phys. Rev. **90**, 169 (1952); **91**, 440 (1953).
[33] J. Marshall, Phys. Rev. **86**, 685 (1952).

limiting β with a Lucite radiator is 0.67) and because of its inherent low background properties. In operating this counter with the photomultiplier cathode in the proton recoil beam, it was found that it had a slight sensitivity for protons below the Čerenkov threshold. This was reduced below measurable limits by a 3-in. thick Cu absorber, R' in Fig. 5.

The monitor telescope was set to observe proton recoils at 20° to the neutron beam. The counters M in Fig. 5 are 1 in.$\times$1 in.$\times\frac{1}{4}$ in. diphenyl-acetylene crystals optically coupled to 1P28 photomultiplier tubes, set 9 in. and 13 in. from the scatterer. R is a 2.5-in. thick copper absorber that limits the sensitivity of the telescope to high-energy recoils. This was done so that the monitor actually monitored the neutron beam used in the experiment, and not stray radiations from the cyclotron that might not be strictly proportional to the neutron intensity. The lead shields S served to reduce singles rates in the counters and also to prevent any influence of the sample, which was not far away, on the monitor.

C. Electronics

Strict linearity of the counting systems was achieved through the use of fast circuits. The accidental coincidence rates were negligibly low because of the fast resolving times of the coincidence circuits, and counting losses were made negligible through the use of high speed, 10-Mc scaling circuits and very moderate counting rates of 15 to 30 per sec.

The signal pulses from the two monitor counters were each amplified by a 200-Mc bandwidth distributed amplifier of voltage gain 10, clipped to 4×10^{-9} sec by shorted cables, and fed into a two-channel, 6BN6 tube coincidence circuit of the type described by Fischer and Marshall.[34] The output of the coincidence circuit was connected directly to a Hewlett-Packard 10-Mc scaling circuit for counting. Since the average counting rate was low, a slow scaler was not needed, and the output of the Hewlett-Packard was connected directly to the mechanical register circuit.

Similarly, the signals from the photomultiplier tubes of the detector telescope were amplified, limited, clipped to 6×10^{-9} sec and connected to a multichannel diode coincidence circuit. The voltage gain used in the two liquid scintillator channels was 10, while that in the Čerenkov counter channel was 300. This fast coincidence circuit, similar to one described by Chen,[35] was designed and built by Fischer of this laboratory. The coincidence output was amplified by two 200-Mc distributed amplifiers, each with a gain of 10, and connected to a 10-Mc scaler.

D. Samples

The hydrogen cross section was obtained from measurements of the attenuation of cyclohexane, benzene, and graphite. Since this technique involved two independent differences, it afforded a valuable check on the values obtained for this important element. The deuterium cross section was obtained from a comparison of the attenuation of samples of equal thickness of heavy and light water. The oxygen, sulfur, and chlorine cross sections were obtained from differences of water and hydrogen, carbon disulfide and carbon, and carbon tetrachloride and carbon, respectively. The remaining eight cross sections were obtained from a study of the attenuation of solid samples of the pure elements.

Great purity of samples is not necessary for even very accurate cross-section determinations, particularly those of medium weight elements, provided actual measured densities are used in the calculations, for since the cross section per nucleon does not change rapidly with mass number, a given weight impurity will not have a greatly different contribution to the cross section than the principal element. Accordingly, commercial purities were considered adequate for the metals studied, though the uranium and thorium samples, loaned by Argonne National Laboratory, happened to be of very high purity, as were the samples of pile graphite used. The liquid samples were all of reagent grade purity, since their use involved differences in the calculation of desired cross sections.

E. Procedure

The chief concerns in the actual running of the experiment were the geometrical alignment of the apparatus, the proper operation of the electronic equipment, and the statistical and systematic errors inherent in the procedure chosen.

The target was designed such that it could be placed in the proton beam reproducibly by remote control; the collimators, being welded to the shield wall, formed a permanently aligned system, and also constituted good visual reference points for the alignment of the entire apparatus. Before each day's run, the detector assembly, consisting of the polyethylene scatterer holder and the counter telescope, was visually aligned. The exact position of the scatterer in the neutron beam was checked by exposing an x-ray film to the beam immediately behind the scatterer holder. Any necessary adjustments having been made, the sample holder was placed in the proper position using the scatterer and the collimators as reference points. A special rolling platform was constructed on which the sample holder was mounted in such a way that it could conveniently be interposed into, and removed from the beam.

During the above set-up operations, the electronic circuits were turned on and allowed to come up to their ambient temperatures, and the photomultiplier voltages were adjusted to assure operation of the scintillation counters on plateaus. Delay curves were taken in the two channels of the monitor and in the three channels

[34] J. Fischer and J. Marshall, Rev. Sci. Instr. **23**, 417 (1952).
[35] T. C. Chen, Proc. Inst. Radio Engrs. **38**, 511 (1950).

of the detector, in the first place to assure that the counters were aligned in time, and in the second place to judge, by the extent to which the curves were of the expected shape and width, that the over-all system, including the coincidence circuit, was operating properly.

Concerning the statistical errors of counting, the over-all accuracy was limited by the total number of counts obtained in the intensity measurements, the errors being minimized by the appropriate apportionment of counting times between observing attenuated and unattenuated intensities, and by the use of optimal thicknesses of sample whenever feasible.[36]

With regard to systematic errors, the chief concerns are with (a) the variations in the relative counting efficiency of the monitor and detector systems and (b) the linearity of these two systems. The adverse effect of the first of these can be held down by counting attenuated and unattenuated beams for short periods alternately. Then, for any steady drift in the efficiencies over a period of hours, the effect on one complete cycle of I and I_0 is minimized, and for any random fluctuations in the efficiencies the effects will tend to average out when the values of many cycles are combined. Thus, possible systematic error from these causes can be converted into a random error which can be reduced by simply taking more data.

Possible deviations from linearity in either of the counting systems are extremely important, though more serious in the case of the detector than the monitor, since any nonlinearity in the detector would lead directly to a misleading estimate of cross section, whereas errors in the monitor would tend to be more random in nature, particularly since data were taken only when the cyclotron beam intensity was quite steady. Over-all linearity of the detector was checked by comparing ratios of I to I_0 obtained with the same sample at different beam intensities. For this purpose the cyclotron intensity was reduced by adjusting only the ion source conditions, leaving the rf system unaltered in order to reduce the possibility of changing the duty cycle factor and thus invalidating this test. No nonlinearities were observed to within the precision of the tests.

III. VALIDITY CONSIDERATIONS

A. Neutron Energy

If the cross sections determined are to be characteristic of a definite neutron energy, it is evident that the beam used should be reasonably monoenergetic, and that its average effective energy should be known. The precise extent of the energy spread allowable can be gauged from the rapidity with which the cross sections appear to vary with energy. Inasmuch as comparison of the present results with those at 280 Mev indicates that the cross sections appear nearly independent of energy in this energy range, the requirements in the direction of a monoenergetic beam are not very stringent for the present experiment.

The energy spectrum of the neutrons from the beryllium target was deduced from range measurements of recoil protons,[37] basing the energies on the range values of Aron.[38] The resulting neutron spectrum is shown as curve A in Fig. 6. A fairly sharp peak is evident at about 400 Mev. However, in view of the uncertainty of the corrections for loss of protons in the absorbers due to nuclear processes, as well as other inherent difficulties in the deduction of high-energy neutron spectra from range measurements, curve A is to be considered of limited reliability in its details, particularly that of the low-energy tail. The relative narrowness of the distribution is similar to that reported for the Carnegie cyclotron,[39] but apparently quite different from the very broad distributions observed at Columbia[40] and at Berkeley.[41]

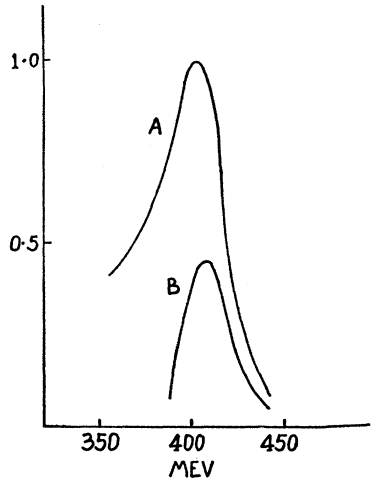

FIG. 6. Neutron energy spectra: A—produced by 450-Mev protons on a 2-in. beryllium target; and B—effective energy spectrum of the neutron beam used in the experiment.

[36] It can be shown, for the case of low background, that the optimal thickness of sample in a transmission measurement is about two mean free paths. Also, the statistical errors can be minimized (for a total time spent counting) if the counting times are apportioned as

$$t/t_0=(I_0/I)^{\frac{1}{2}} \quad \text{and} \quad t_B/t=(I_B/I)^{\frac{1}{2}},$$

where t, t_0, and t_B are the counting times of the attenuated, the unattenuated, and background intensities, I, I_0, and I_B, respectively.

[37] The neutron spectrum shown here is a composite of the results of three independent unpublished measurements at this laboratory: Marshall and Nedzel, range in Pb, and Nedzel, range in Cu, both observations made at 10° to the neutron beam on recoils from polyethylene; G. Yodh, range in Cu using recoils at 20° from a liquid hydrogen target. The three neutron spectra deduced from these range measurements agreed within 10 Mev on the energy of the maximum and of the end point of the distribution, but yielded relatively poor agreement on the low-energy tail.

[38] W. A. Aron, University of California Radiation Laboratory Report UCRL-1325, 1951 (unpublished).

[39] A. J. Hartzler and R. T. Siegel, Phys. Rev. **90**, 362 (1953).

[40] Goodall, Loar, Durbin, and Havens, Phys. Rev. **89**, 724 (1953).

[41] Cladis, Hadley, and Hess, Phys. Rev. **86**, 110 (1952).

The neutron spectrum having a fairly well defined high-energy limit, the spread of the effective beam can be set by cutoff at the low energy and through the action of a threshold detector. The effective spectrum for the present experiment was determined empirically by measuring the range of the protons actuating the detector, making suitable corrections for the stopping power of the counter itself. In addition, the residual range of the recoils above the threshold of the detector was measured by interposing absorbers between the first two of the three counters of the telescope. These measurements yielded the effective energy spectrum B of Fig. 6. Although this is not a very precise determination, inasmuch as the entire extent of the distribution was only 60 Mev, it permitted an entirely adequate estimate of the mean effective neutron energy for the purposes of this experiment. This mean effective neutron energy was determined as 410±20 Mev.

B. Tests of Exponential Attenuation

The significance of a definition of cross section independent of the amount of attenuating material rests on the exponential nature of attenuation. There is little question that a beam of neutrons of a given energy will exhibit pure exponential attenuation in an ideal good geometry experiment. Therefore, one good check on the validity of the experiment would be a measurement of the attenuation over a wide range of thicknesses of absorber. The presence of a background counting rate or any nonlinearity in the detector system would show up as a deviation from the expected exponential attenuation.

TABLE I. Deviations of the observed attenuations from those expected on the basis of measurements made with absorbers of about two mean free paths thickness.

Thickness in mean free paths	Deviation of I/I_0	Precision of I/I_0
0.456	− 0.3%	0.5%
0.458	− 0.7%	1.2%
0.762	+ 0.6%	1.6%
0.890	+ 0.9%	1.1%
0.916	− 0.7%	1.7%
1.030	− 1.0%	1.2%
1.118	− 0.6%	1.5%
1.190	+ 0.8%	1.0%
4.27	+ 6%	10%
6.46	−10%	20%

Most of the elements were studied in samples of several thicknesses, the largest being about two mean free paths in each case. The observed attenuations for the thinner samples are the points plotted at the upper left of Fig. 7. The straight line drawn is the expected attenuation on the basis of measurements with two mean free path thick samples. In order to extend this test of exponentiality into a region of greater thicknesses, two measurements of attenuations, at four and at six mean free paths, were made with lead absorbers especially for this purpose. Table I gives the deviations and the precision of determination (the statistical error) of each point. No systematic deviation beyond the accuracy of measurement is evident.

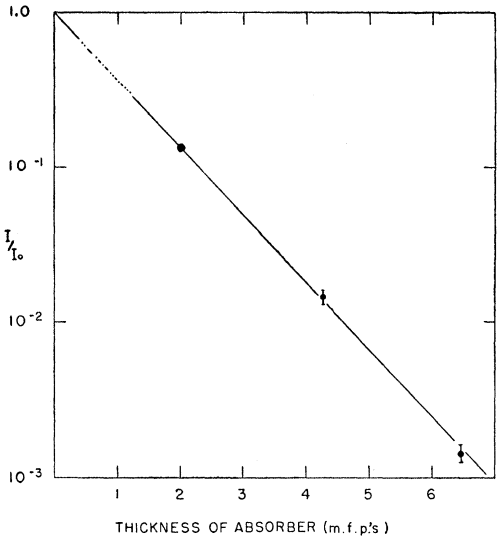

FIG. 7. Transmission of the neutron beam *vs* number of mean free paths thickness of absorber. Points are plotted for the attenuation of samples of all elements for which more than one thickness was studied. Normalization was in terms of the two mean free path thick samples. No background rates were subtracted, whence the strict exponential nature of the attenuation apparent is an indication of the negligibly low background achieved in this experiment.

C. Corrections

Few and only small corrections had to be applied to the observed rates. The accidental coincidence rates were always negligible, and hence no corrections were required for this factor.

A correction was applied for finite geometry, taking into account the scattering of neutrons into the detector by the sample in the same general fashion as described by Cook *et al.*[12] Tests conducted provided an approximate verification, at least in the upper limit, of this correction factor. In the present experiment, this correction for finite geometry amounted to only 1 percent in cross section for uranium, and less for other elements, being proportional to the cross section for the same geometry.

In the case of the liquid samples a correction had to be applied for the attenuation by the aluminum windows of the sample holders. This was calculated from the measured aluminum cross section, and amounted to 1.1 percent in attenuation.

D. Errors

The statistical errors of counting were the predominant source of uncertainty in the case of all cross sections measured. However, the deviations of individual counts were not observed to be significantly outside of the expected standard deviations. Accidental coinci-

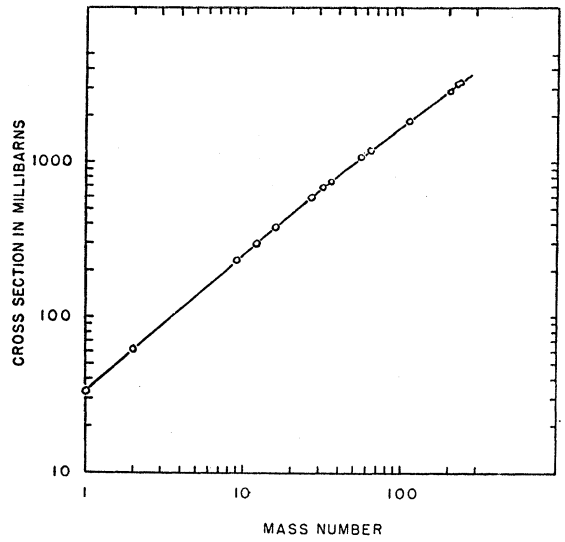

FIG. 8. The total cross sections observed in this experiment.

dence rates were negligible, no counting losses were detected, and over-all linearity tests always indicated linearity within the statistical accuracy of these observations, which was better than 0.3 percent in I/I_0 ratio. No short term variations, outside of statistics, were observed in the relative detector-monitor efficiencies. Slow drifts as great as 5 percent in twelve hours did occur, which were not important for the present experiment, since the amount of change during the relatively short interval of one cycle of observations was entirely negligible. The physical dimensions and weights of the samples were measured accurately, the densities and thicknesses of the solid samples being known to better than 0.3 percent in all cases, and those of the liquid samples to be better than 0.1 percent. The densities of the liquids were determined at the same temperature as that at which they were used.

IV. RESULTS AND CONCLUSIONS

The results of the cross-section measurements of the present experiment are shown as a function of mass number in Fig. 8. The numerical values are presented in Table II, with adjacent columns listing the published cross sections at 280 Mev[18] and 270 Mev,[17] the highest energies previously reported. Comparison reveals that for the heavy elements, the cross sections do not appear to be significantly different at 410 Mev from the values at the lower energies; for the lighter elements, except for the hydrogen cross section, the present work yields somewhat higher cross sections.

A. Hydrogen and Deuterium

The hydrogen cross section was deduced from measurements of the attenuation of samples of cyclohexane, benzene, and graphite, containing approximately the same number of carbon atoms per cm^2. These attenuations were self-consistent, as evidenced in Fig. 9, where they are plotted against moles of hydrogen per cm^2. The straight line drawn corresponds to a hydrogen cross section of 33.7 mb. Observations with these liquid samples also yielded a carbon cross section of 297±3 mb, in good agreement with the 297.5±2 mb value obtained from measurements on graphite.

The *n-p* total cross section at 410 Mev appears somewhat lower, while the deuterium cross section appears higher, than the weighted averages of these same cross sections measured at 270 and 280 Mev; the two sets of values, however, can almost be considered the same within their estimated accuracies. If one

TABLE II. Summary of results. The fourth column represents the results of the present study, at 410 Mev. The published cross sections at 280 Mev and 270 Mev, the highest energies previously reported, are given for comparison in the fifth and sixth columns. The third column gives the radius of the opaque nucleus $(\sigma/2\pi)^{\frac{1}{2}}$ that would give the observed cross section in each case, while the two sets of R, F, and σ columns give the radii, the opacity ($F=\sigma/\pi R^2$), and the cross sections predicted by the two formulas discussed in the text.

Element	$A^{\frac{1}{3}}$	$(\sigma/2\pi)^{\frac{1}{2}}$ (cm×10^{-13})	σ(410 Mev) mb	σ(280 Mev) mb	σ(270 Mev) mb	Formula (3) R (cm×10^{-13})	Formula (3) F	Formula (3) σ mb	Formula (7) R (cm×10^{-13})	Formula (7) F	Formula (7) σ mb
H	1.00	0.73	33.7±1.3	33±3	38±1.5	1.20	0.70	32	1.23−	0.68	32
D	1.26	0.99	62±4	49±5	57±3	1.51	0.84	60	1.55	0.80	60
Be	2.08	1.92	231±4	225±4	229±3	2.50	1.18	231	2.56	1.12	230
C	2.29	2.17	297±3	279±4	288±3	2.75	1.25	298	2.82	1.18	296
O	2.52	2.45	378±5	380±8	372±7	3.02	1.33	381	3.10	1.25	377
Al	3.00	3.06	587±7	566±18	555±8	3.60	1.45	591	3.69	1.37	584
S	3.18	3.27	672±9			3.81	1.49	682	3.91	1.40	672
Cl	3.29	3.44	742±9			3.94	1.51	740	4.05	1.42	734
Fe	3.82	4.13	1073±12			4.60	1.62	1071	4.70	1.52	1056
Cu	3.99	4.34	1187±14	1190±20	1145±15	4.79	1.64	1182	4.90	1.54	1165
Cd	4.83	5.42	1848±21			5.79	1.75	1841	5.94	1.65	1822
Pb	5.92	6.78	2890±30	2890±30	2840±30	7.10	1.85	2915	7.29	1.74	2910
Th	6.14	7.16	3210±40			7.36	1.86	3170	7.55	1.76	3150
U	6.20	7.18	3230−40	3140±50	3290±30	7.44	1.86	3240	7.63	1.76	3220

assumes that the deuterium cross sections at these energies can be considered simply as the sum of the n-p and n-n cross sections, then the 410-Mev data give $\sigma(n\text{-}n)=28\pm4$ mb while the lower energy data yield 19 ± 3 mb.

B. Comparison with Proton Cross Sections

The total neutron cross sections may be compared with the total (nuclear) proton cross sections measured at 408 Mev.[42] These are given in Table III. [The value of the neutron cross section listed for lithium was interpolated by calculation from the empirical formula (3) given below, fitted to the neutron cross sections.] The comparison shows evidence for support of the charge symmetry hypothesis.

C. Empirical Formula

It was suggested by Fermi in a private communication that the formula

$$\sigma=2\pi R^2[1-\exp(-KR)], \tag{3}$$

where $R=r_0A^{\frac{1}{3}}$, be fitted to the data, in order to allow approximately for the transparency of nuclei for neutrons. A best fit was obtained for

$$r_0=1.20\times10^{-13}\text{ cm},\quad K=0.360\times10^{13}\text{ cm}^{-1}. \tag{4}$$

Using the above values of the parameters, the cross sections of all the elements studied were calculated, the results being given in Table II in the column labeled "σ" under the formula (3) heading. The values of R shown under this same heading were calculated from $r_0A^{\frac{1}{3}}$; the F values are the ratios of these cross sections to the "geometrical cross section," i.e., $F=\sigma/\pi R^2$, which might be termed the nuclear opacity and has the value two for an opaque nucleus. Comparing the cross sections computed from this formula with the measured values, surprisingly close agreement is evident, the formula values being identical to the measured values within the accuracy of determination of the latter, except in the case of hydrogen.

The function (3) is plotted as curve A in Fig. 10, the points shown on it being the experimentally observed cross sections plotted according to the choice of parameters (4).

TABLE III. Comparison of total nuclear cross sections of various light elements for neutrons and for protons.

Neutron cross sections (mb)			Proton cross sections (mb)		
n-p	(H)	33.7 ± 1.3	p-n	(D-H)	$31.6+2$
n-n	(D-H)	28 ± 4	p-p	(H)	24 ± 1
	Li[a]	186		Li	194 ± 8
	Be	231 ± 4			242 ± 6
	C	297 ± 3			285 ± 14
	O	378 ± 5			406 ± 3

[a] Interpolated from empirical formula.

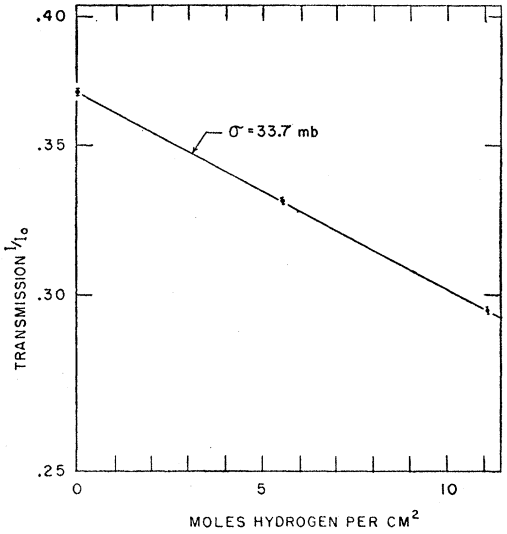

FIG. 9. Attenuation of the neutron beam by hydrogen. The plotted points are the observed transmissions of samples of graphite, benzene, and cyclohexane, respectively, all samples containing the same surface density of carbon.

D. Nuclear Radii

The cross-section data can be used to compute the radii on the basis of the opaque nucleus model, as given by Eq. (2). The values of the radius, $(\sigma/2\pi)^{\frac{1}{2}}$, and of $A^{\frac{1}{3}}$ are shown in Table II, and a plot of these data is given in Fig. 11. It is seen that, except for

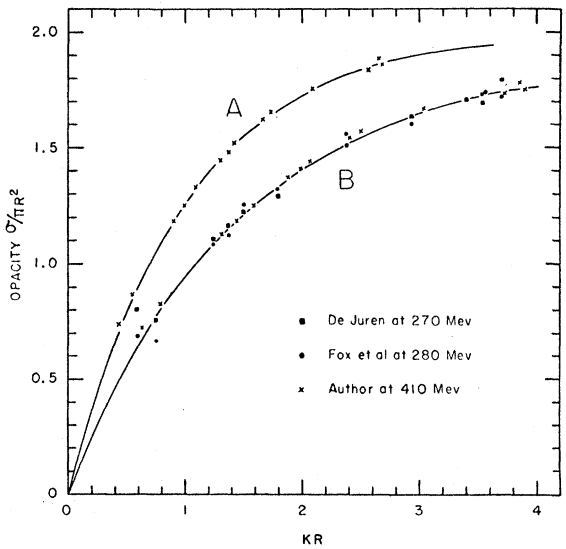

FIG. 10. The opacity of nuclei to neutrons *vs* the product of the nuclear radius R and the absorption coefficient K of neutrons in nuclear matter—curve A, as predicted by the empirical formula (3), and curve B, as predicted by the transparent optical model when $k_1=0$. The plotted points are the experimental data to which these functions were fitted.

[42] Marshall, Marshall, and Nedzel, Phys. Rev. **91**, 767 (1953).

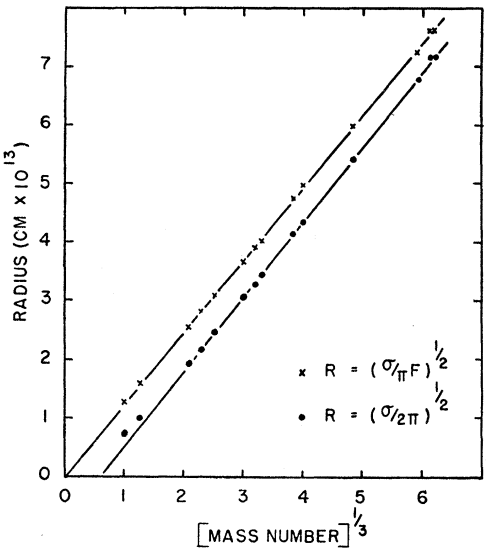

FIG. 11. The points along the lower straight line are the radii of the equivalent opaque nucleus; *viz.*, $R=(\sigma/2\pi)^{\frac{1}{2}}$; the points along the upper straight line are the radii calculated from the observed cross sections on the basis of the fit (8) to the transparent optical model; *viz.*, $R=(\sigma/\pi F)^{\frac{1}{2}}$, where F is the nuclear opacity.

hydrogen and deuterium, the points fall quite closely on a straight line in the form of (2), where $r_0=1.27\times10^{-13}$ cm and $a=-0.73\times10^{-13}$ cm. These values at 410 Mev can be compared with those reported for 280 Mev,[18] *viz.*, $r_0=1.27\times10^{-13}$ cm and $a=-0.82\times10^{-13}$ cm, and with those which can be fitted to the 153-Mev data, $r_0=1.39\times10^{-13}$ cm and $a=-0.86\times10^{-13}$ cm.

Since the phenomenon of negative intercepts of (2) revealed above is not readily explainable in terms of an opaque nucleus, it is of some interest to examine the applicability of the transparent optical model of Fernbach, Serber, and Taylor. This model predicts, for the absorption and diffraction cross sections,[43]

$$\sigma_a=2\pi\int_0^R[1-\exp(-2Ks)]sds$$

$$=\pi R^2[1-\{1-(1+2KR)\exp(-2KR)\}/2K^2R^2]; \quad (5)$$

$$\sigma_d=2\pi\int_0^R|1-\exp(-K+2ik_1)s|^2\rho d\rho, \quad (6)$$

where R is the radius of the nucleus (again, $R=r_0A^{\frac{1}{3}}$), s is the distance traversed through the nucleus by the neutron, and ρ is the distance from the center of the nucleus. An expression for σ_d has been given analytically[15] in terms of R, K, and k_1, but it is rather long to reproduce here.

[43] It is to be noted that the absorption cross section σ_a as used here refers to all inelastic processes; the diffraction cross section σ_d then refers to all elastic processes.

[44] S. Fernbach, University of California Radiation Laboratory Report UCRL-1382 (unpublished).

As was the case at 280 Mev,[44] it was found that observed cross sections were best fit when $k_1=0$. For this case the expression for the total cross section reduces considerably; *viz.*, the sum of σ_a and σ_d from (5) and (6) becomes

$$\sigma=\sigma_a+\sigma_d$$
$$=2\pi R^2\{1-2[1-(1+KR)\exp(-KR)]/K^2R^2\}, \quad (7)$$

shown as curve B in Fig. 10. This equation was fitted to the data assuming r_0 and K independent of mass number, a best fit being obtained for

$$r_0=1.23\times10^{-13}\text{ cm} \quad \text{and} \quad K=0.51\times10^{13}\text{ cm}^{-1}. \quad (8)$$

The cross sections calculated from formula (7) are shown in Table II, and the agreement of the formula with the experimental values is indicated in Fig. 10. Nuclear radii calculated from the measured cross sections on the basis of (7) are plotted in Fig. 11, where they are seen to fall closely on a straight line, passing through the origin when plotted against $A^{\frac{1}{3}}$, as is required for constant nuclear density.

However, this particular choice of values of the parameters, though it gives the correct A dependence of the cross sections, is not entirely satisfactory from the point of view of the transparent optical model. K is presumably the absorption coefficient of neutrons in nuclear matter and should be given in terms of the nucleon interactions by

$$K=\frac{3}{4\pi r_0^3A}[Z\sigma_{np}+(A-Z)\sigma_{nn}]. \quad (9)$$

If one uses the aforementioned choice of r_0, the value of σ_{np} of 34 mb observed from this work, and $\sigma_{nn}=\sigma_{pp}=24$ mb from the measurements at 408 Mev, and further assumes that these cross sections for free nucleons apply fully to bound nucleons, then (9) gives $K=0.36\times10^{13}$ cm^{-1}, a value considerably less than that required to fit the A dependence of the cross sections. This particular difficulty could be related to the assumption of nuclear density independent of A and would be less serious if the density were larger for heavier nuclei.

One would expect the optical model to apply more rigorously to the heaviest nuclei. K can be calculated according to (9) and then r_0 determined by fitting to measured cross sections. Using the cross sections of Pb, Th, and U, one obtains $r_0=1.35\times10^{-13}$ cm and $K=0.274\times10^{13}$ cm^{-1}. This choice of parameters, however, predicts cross sections 10–15 percent too low for light elements.

Thus, if one requires nuclear radii to be strictly proportional to $A^{\frac{1}{3}}$, the transparent optical model can be made to fit the observed dependence of the total cross sections on mass number very well, but not for values of the absorption coefficient expected on the basis of its definition.

E. Comparison to Cross Sections at 270–280 Mev

The cross sections at 410 Mev can be compared in a systematic way with those at 270–280 Mev by fitting the latter to (7) in the same manner as was done with the former, and comparing the parameters in the two cases. This comparison may be of interest even if the interpretation of the parameters themselves is in question. A fit is obtained[45] for

$$r_0 = 1.23 \times 10^{-13} \text{ cm} \quad \text{and} \quad K = 0.485 \times 10^{13} \text{ cm}^{-1}. \quad (11)$$

The 270- and 280-Mev cross sections[17,18] are plotted in Fig. 10 to illustrate the quality of the fit. By comparing (11) with (8), it is to be noted that K is about 5 percent larger at 410 Mev. On the basis of the definition (9) of K, this systematic difference could be explained by an average increase of the nucleon-nucleon cross sections in that amount. There is evidence for this in the higher value obtained for the deuterium cross section at 410 Mev, but the probable errors are too large to make the comparison completely convincing. The neutron cross sections already discussed seem to deny that the n-p cross section is rising, but again there is an appreciable probable error. As to the n-n cross section, one can again assume equality with the nuclear part of the p-p cross section. Comparison of the total cross sections at the two energies is difficult because of the present ambiguous status of the available data. However, there there is some evidence[46] that the elastic part of the nuclear p-p cross section remains constant in this energy range, while the meson production rises to about 2–3 mb at the higher energy.

[45] This choice is different from that of Fernbach, reference 44 (*viz.*, $r_0 = 1.39 \times 10^{-13}$ cm and $k = 0.25 \times 10^{13}$ cm^{-1}) because here the formula of the optical model is fitted as an empirical formula, whereas in the other, both theoretical and experimental considerations influenced the choice of the parameters.

[46] Marshall, Marshall, and Nedzel, Phys. Rev. **91**, 767 (1953); **92**, 834 (1953).

In conclusion, the principal results emerging from this study may be summarized as follows: (1) Compared to the previously published values at 270 and 280 Mev, the 410-Mev cross sections tend to the same values for the heavier nuclei, but to values several percent higher for the lighter nuclei (excluding hydrogen and deuterium); (2) a formal application of the formula from the transparent optical model permits a good fit to the mass dependence of the cross sections (even with the requirement of constant nuclear density), but leads to values of the absorption coefficient in nuclear matter inconsistent with the definition of the latter quantity in terms of this model, thus creating an ambiguity in the interpretation of the determined nuclear radii; (3) a simple two parameter empirical formula was found to fit the 410-Mev cross sections to within the estimated accuracy of their determination; (4) comparison of the measured neutron cross sections with proton cross sections supports charge symmetry.

The author wishes to express his appreciation to Professor John Marshall for his suggestion of the work and for his guidance and help during the course of the experiment; to Professors S. K. Allison and H. L. Anderson for their encouragement of the work; and to Professor R. H. Hildebrand for many valuable discussions and for his help in procuring special materials for the experiment. Thanks are also given to Mr. Joachim Fischer for his assistance with the electronics, particularly for his construction of the multichannel coincidence circuit used, and to Mr. Lester Kornblith and the members of the cyclotron crew for their friendly cooperation during the many hours of running required for this study. Grateful acknowledgment is made to the Argonne National Laboratory of the U. S. Atomic Energy Commission for the loan of the thorium, uranium, and heavy water samples used.